Structural characterization and the sorption properties of the natural and synthetic zeolite

C. ORHA[a,b*], A. POP[c], C. LAZAU[b], I. Grozescu[b], V. TIPONUT[a,c], F. MANEA[c]
[a]*National Institute for Research and Development in Microtechnologies, Bucharest, Romania*
[b]*National Institute for Research and Development in Electrochemistry and Condensed Matter, Timisoara, Condensed Matter Department, P. Andronescu Street, 300254, Timisoara, Romania*
[c]*"Politehnica" University from Timisoara, P-ta Victoriei Street, 34206, Timisoara, Romania*

The goal of the present work was to study the sorption of humic acids (HA) from water on natural and synthetic zeolite A envisaging the drinking water treatment. Synthetic zeolite A nanoparticles were synthesized from natural clinoptilolite as Si source and sodium aluminate as Al source. In comparison with natural zeolite, synthetic zeolite A exhibited well defined pore sizes, which confer it a higher adsorption capacity. The comparative surface characterization of both natural and synthesized zeolites has been investigated by X-ray diffraction (XRD), scanning electron microscope (SEM)/ EDX analysis and FT-IR spectroscopy.

(Received March 21, 2011; accepted May 25, 2011)

Keywords: Natural zeolite, Synthetic zeolite, Humic acid, Adsorption

1. Introduction

Natural zeolites are hydrated aluminosilicates based on an infinite three-dimensional structure of tetrahedrons as TO_4 (T = Si, Al, B, Ge, Fe, P, Co) joined by oxygen atoms [1]. Clinoptilolite is the most abundant natural zeolite and is mainly found in specific types of sedimentary rocks in the form of small crystals (0.1–100 μm) associated with clays and other silicate and aluminosilicate phases of similar density. The crystals of clinoptilolite accommodate two different systems of micropores interconnected within the lattice, capable of hosting extra-framework, i.e., exchangeable cations (Na^+, K^+, Ca^{2+}, Mg^{2+}) in association with mobile H_2O molecules.

Synthetic zeolite A with the ideal chemical composition of $Na_{12}[(AlO_2)_{12}\ (SiO_2)_{12}]\cdot 27H_2O$, can be prepared using hydro-gel of various type of Si and Al precursors such as sodium silicate, sodium aluminate and other minerals such as clays and natural zeolites under hydrothermal condition [2]. This zeolite is one of the most important molecular sieves, and has a good cation exchange capacity and can easily exchange sodium ion with cations. Nanocrystalline zeolites have unique properties in comparison to conventional micrometer-sized zeolite crystals because these materials have been reduced in size to just a few unit cells, this gives significant change in properties [3].

Zeolite materials allow an introduction of new functional groups through several processes of modification, improving substantially its activity and selectivity on the removal several substances [4]. Many authors show the use of zeolite on environmental applications, mainly organic pollutants removal from effluents by adsorption processes [5-7].

Natural organic matter (NOM) is part of all aquatic systems [8]. Humic substances including humin, humic and fulvic acid (HA and FA) are the major components of NOM. They are formed during the decomposition of plant and animal biomass in natural systems and usually include a skeleton of alkyl and aromatic units with functional groups such as carboxylic acid, phenolic hydroxyl, and quinone groups attached to them. In drinking water, presence of NOM will cause several problems such as the colour and nasty odour, the formation of disinfection by-products and its complexation with heavy metals, they can act as a major foulant affecting various applications of membrane processes due to compete with low-molecular-weight synthetic organic chemicals, as well as inorganic pollutants, reducing their adsorption rates and equilibrium capacities [9]. Many methods have been adopted to remove humic substances from drinking water: coagulation/flocculation separation, ion exchange, adsorption on zeolite or activated carbon and membrane filtration [10].

The goal of this study is synthesize nano-sized zeolite using natural clinoptilolite rich tuff to improve its performance to remove humic acid (HA) from aqueous solution by adsorption process. The comparative adsorption capacities of natural and synthetic zeolite for humic acid (HA) removal from aqueous solution were investigated. Also, the structure and the morphology of synthetic zeolite was characterised in comparison with natural zeolite through X-ray diffraction, SEM/EDX analysis and FT-IR spectroscopy.

2. Experimental

2.1. Preparation of synthetic zeolites

Synthetic zeolites (ZA) were synthesized from natural clinoptilolite as Si source.

Natural zeolite with high clinoptilolite content was supplied by Cemacon Company, Romania. The mass composition of powder zeolitic mineral was: 62.20% SiO_2, 11.65% Al_2O_3, 1.30% Fe_2O_3, 3.74% CaO, 0.67% MgO, 3.30% K_2O, 0.72% Na_2O, 0.28% TiO_2.

A solution of natural clinoptilolite, sodium hydroxide and water with 1:5:50 mass ratios were mixed for 1 hour at 90 °C (solution I). The aluminum solution was prepared from sodium aluminate, sodium hydroxide, sodium aluminate and water with 1:1.5:7.8 mass ratios, were mixed and heated to make a clear solution (solution II). The solutions II and I with 1:6.9 mass ratio were mixed together. Then, the mixture was heated at 90 °C and stirred with a mixing rate of 1000 rpm for 2 hours. The synthetic zeolite was thermally treated at 105°C for 8h for a good cristallinity

2.2. Adsorption experiment

In this study the commercial humic acid provided by Fluka was used. The molecular structure of humic acid is represented in Fig.1.

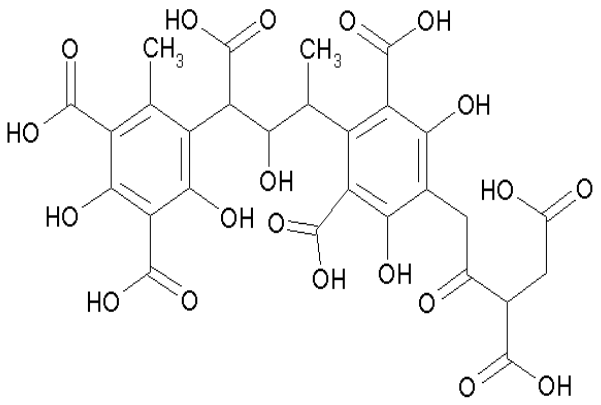

Fig.1. Molecular structure of humic acid

The adsorption of HA on natural and synthetic zeolite A was studied using batch method. 100 mL solutions of HA at different initial concentrations (10, 15, 25 mg·L^{-1}) were kept in contact with 0.2 g zeolite, under continuously stirring at 25°C for 120 min, in the dark. The pH was adjusted to 5 using 10% H_2SO_4 solution. The initial concentrations of HA solutions were prepared from a stock solution of 100 mg·L^{-1}.

At different time intervals (5, 10, 15, 20, 30, 60, 90 120 min), samples were collected and the extent of adsorption of the HA on the zeolite surface was evaluated as HA removal efficiency. All HA concentrations were measured with a UV-vis spectrophotometer (Varian Carry 100) at 254 nm. HA concentrations were measured by constructing calibration curves between tabsorbance recorded at 254 nm and concentrations. Prior to analysis, samples were filtered through a Milipore filter (pore size 0,45 μm) in order to remove the zeolite from the aqueous solution.

The adsorbed HA amount (qe) per unit adsorbent mass was calculated based on equation (1):

$$q_e = \frac{(c_0 - c_e)V}{m} \quad (1),$$

where: c_o is the initial HA concentration, c_e is the concentration of HA at equilibrium (mg/L), m is the adsorbent mass (mg) and V is the solution volume (L).

2.3. The materials characterization

The crystallinity of the prepared samples was measured by X-Ray diffraction (XRD) using PANalytical X'PertPRO MPD Difractometer with Cu tube. A scanning electron microscopy (SEM) using Inspect S PANalytical model coupled with the energy dispersive X-ray analysis detector (EDX) was used to characterize the external surfaces of the hybrid materials, using catalyst powder supported on carbon tape. The FT-IR spectra were recorded in KBr pellet for solid compounds with a FTIR–PRESTIGE 21 Shimadzu instrument.

3. Results and discussion

3.1. XRD analysis

The XRD patterns of natural zeolites are illustrated in figure 2a. The presented results revealed that the natural zeolite used is mostly clinoptilolite (2 theta: 10º; 22.5º; 30º). The presence of other crystalline compounds, e.g., mordenite, quartz and illite is also revealed [11].

The XRD spectra of synthetic zeolite ZA provided in Fig. 2b confirm that the synthetic zeolite is LTA with a good crystallinity. Because the natural zeolite was the raw material for the synthetic one, the presence of clinoptilolite is obvious in XRD patterns [2].

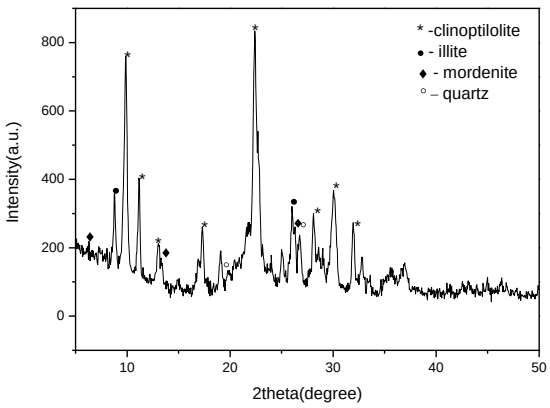

a)

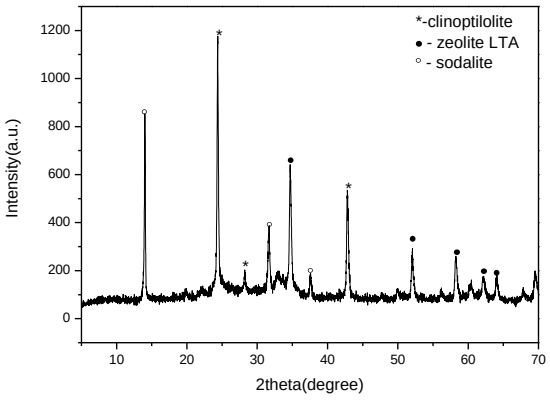

b)

Fig. 2. XRD pattern of a) natural zeolite ZN; b) synthetic zeolite ZA

3.2. Scanning electron microscopy (SEM) and Energy Dispersive X-ray Analysis (EDX) results

In Fig. 3 is presented the image of natural powder zeolite ZN. According to the literature data the crystals of these materials have characteristic monoclinic symmetry of blades and laths, some of which are similar to the coffin shape of megascopic heulandite that occurs in vugs in basalts [12,13].

Fig. 4 present the SEM image of the synthetic zeolite ZA. The surface morphology of synthetic zeolite is similar to natural zeolite. In comparison with natural zeolite, for which the particles size ranged between 4-11 μm and the particles size of the synthetic zeolite A was in the range 20 to 300 nm, and the SEM images showed a more uniform structure with smooth edged lamellar crystals. EDX spectra provided a semiquantitative elemental analysis of the surface indicating that Al, Si and Na were present on the synthetic zeolite surface and the Si/Al ratio was 1.0-1.14. For comparison, the presence of the major elements such as Na, Si, Al, Ca, K, Mg can be seen from the EDX spectra, and Si/Al ratio of 4-5.

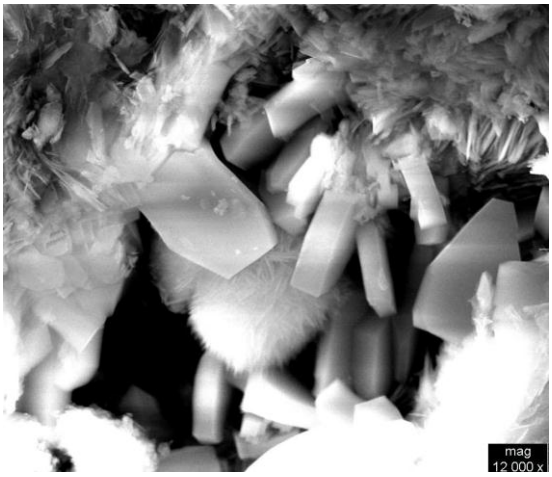

Fig. 3. SEM image for natural zeolite ZN

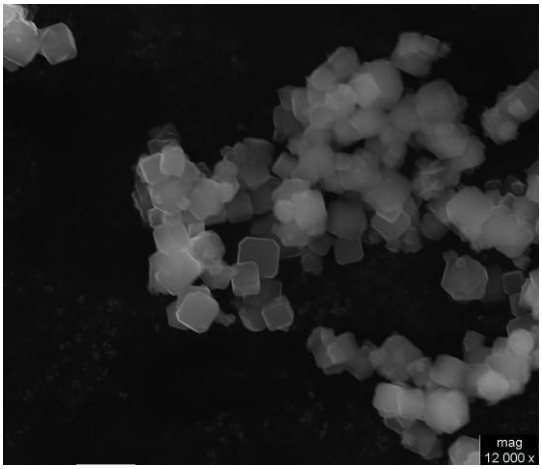

Fig.4. SEM image for synthetic zeolite ZA

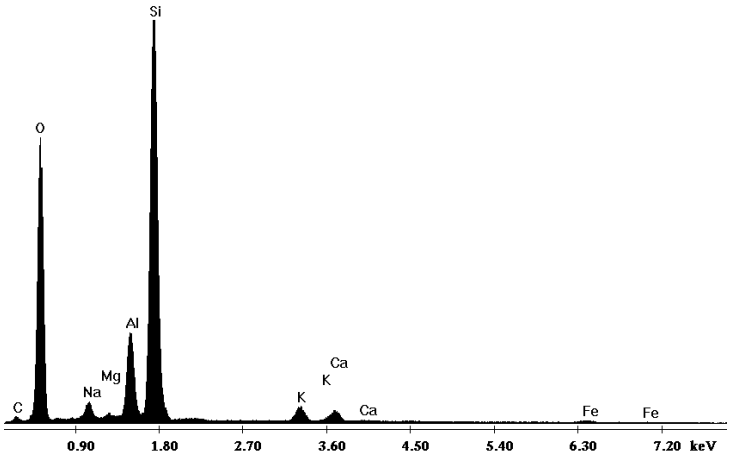

a)

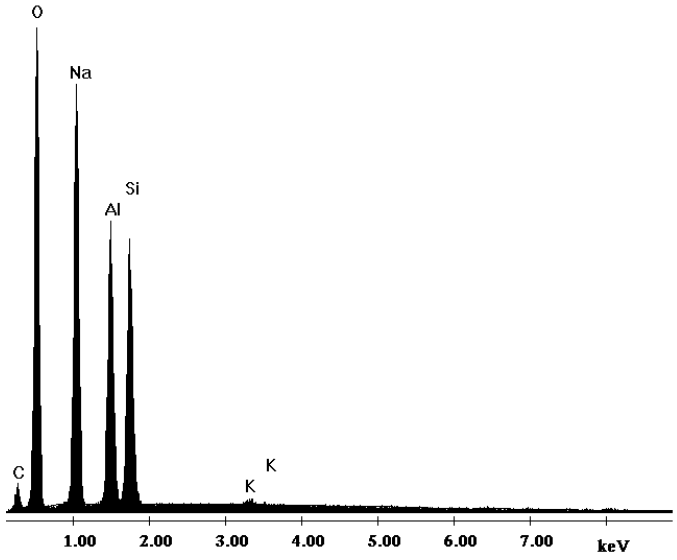

b)

Fig.5. EDX of natural zeolite a) and synthetic zeolite b)

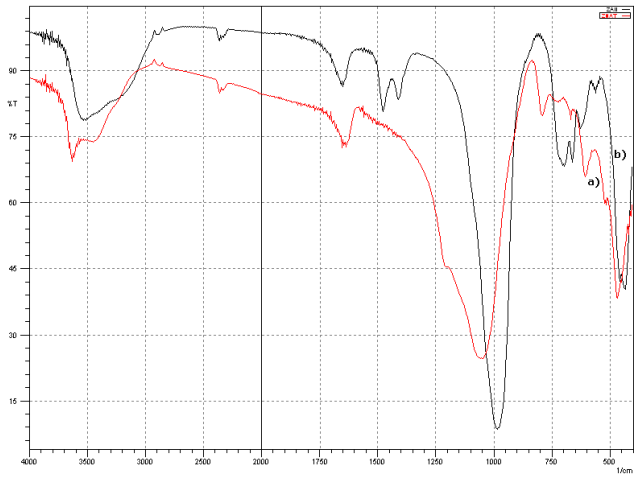

Fig.6. FT-IR spectra of a) natural zeolite ZN and b) synthetic zeolite ZA.

The stretching and bending modes (absorption characteristics) of the T-O units (T = Si or Al) in zeolite framework are noticed from FT-IR spectrum (Fig.6).

The absorption bands at 500, 450 cm^{-1} characteristic to T-O bending vibrations are shifted to lower frequencies for synthetic zeolite due to the Si/Al ratio which is more smaller comparative to natural one [14,15].

For both the natural and synthetic zeolite, the FT-IR spectrum shows the band characteristic to zeolite rings in the range of 400-800 cm^{-1}. The 4-4-1 complex shows the most complicated structure among all zeolites because in this complex both the 4 membered rings as well as 5-membered rings occur. For natural zeolite the bands in the range of 590-610 cm^{-1} probably arise from the 5 membered ring vibrations, but for syntetic zeolite ZA the band in the 548-578 cm^{-1} regions is related to the presence of the double rings in the framework structure [16]. The presence of the week bands in the range 660-670 cm^{-1} can results from the vibrations of higher numbers of ring

members in the case of ZN [17], and for synthetic zeolite ZA, stretching modes involving the tetrahedral atoms were assigned in the region of 677-719 cm^{-1}.

The band at 1630–1640 cm^{-1} (Lewis sites) region is assigned to the zeolitic water in the channels of the zeolite [18]. The best spectroscopic method for studying water is to examine the H–O–H bending mode centered near 1630 cm^{-1}. The reason for this is that in IR spectroscopy, the very intense hydroxyl stretching frequencies of water, in this case, play the hydroxyl stretching frequencies of the zeolite.

The slight differences between the bands corresponding to the natural and synthetic zeolite in the range 3400 cm^{-1} and 3600 cm^{-1} atributed to the assymetric and antisymmetric streching mode of molecular water coordinated to the edges of the zeolite channels [19, 20] can be noticed. In addition, for nanocrystalline zeolite it can be observed the absorption band at 3640 cm^{-1}, which is assigned to hydroxyl groups attached to Na^{+} [21].

3.3. Adsorption studies

In general, the large internal surface area of micro- and mesoporous materials leads to a relatively high sorption capacity of the materials toward guest compounds. The sorption capacity can be improved by avoiding diffusional limitations based on the pore size. In zeolite nanocrystals, the diffusion paths are shorter. Figs 7 a) and b) show the results of adsorption experiment for HA, which were conducted comparatively on natural ZN and synthetic zeolite ZA over a HA concentration range between 10 and 25 mg/L. The maximum HA concentration was chosen based on real HA content in surface waters. As can be seen, a complete adsorption of HA on natural zeolite was not observed over a 2 hours adsorption period, while a complete adsorption of HA on synthetic zeolite A occurred after first minutes of adsorbtion.

Under these concentrations range, the both adsorbent allowed that the adsorption process to reach the equilibrium in the same time independent on the HA concentration. However, synthetic zeolite ZA allowed reaching equilibrium faster. Also, the HA removal efficiencies were very high (higher than 90%) for all studied HA concentrations, in comparison with those obtained for natural zeolite ZN, with the HA removal efficiencies ranged of 17 and 42%, depending on HA initial concentration.

From Fig. 7a can be seen that using natural zeolite adsorbent and HA concentration increasing led to lower HA removal efficiency. On the contrary, the slight better HA removal efficiencies were achieved at HA concentration increasing using synthetic zeolite ZA. Based on the above-presented results, it can be concluded that under these HA concentrations range, all added HA were adsorbed on synthetic zeolite ZA indicating an incomplete surface coverage.

The adsorbed HA amount on both types of zeolites for the three HA concentrations are gathered in Table 1.

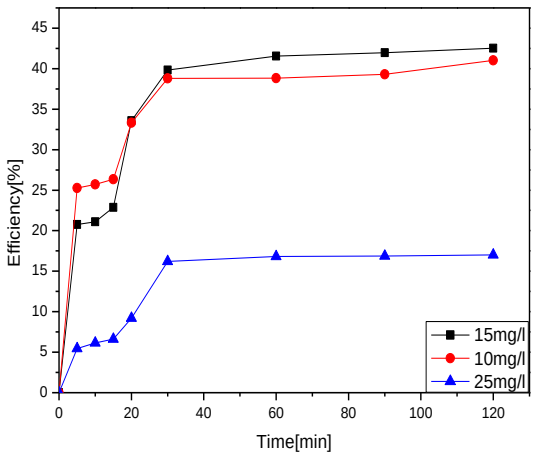

Fig.7. a) Effect of HA initial concentration on HA removal efficiency using natural zeolite ZN adsorbant

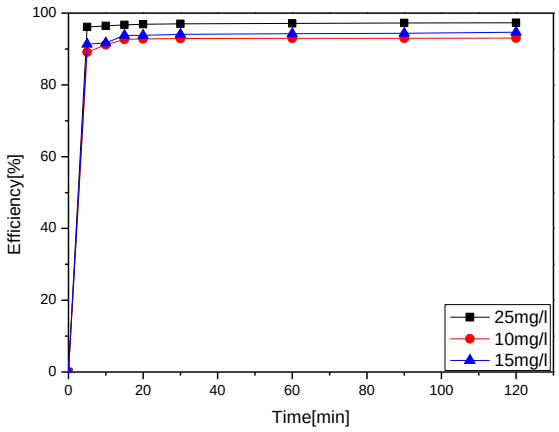

Fig. 7. b) Effect of HA initial concentration on HA removal efficiency using synthetic zeolite ZA adsorbent

Table 1. The comparative adsorption capacities of both natural and synthetic zeolite for humic acid from water

C_0(mg/L)	C_e(mg/L)		q_e(mg/L)	
	ZN	ZA	ZN	ZA
23.96	16.83	0.84	3.56	11.56
13.40	8.06	0.79	2.67	6.30
10.03	6.14	0.71	1.94	4.66

The HA amount adsorbed on both types of zeolite increased with HA concentration increasing, and the best one was achieved for the synthetic zeolite A at 25 mg/L HA. As a result of the experimental adsorption studies, it is seen that very high efficiency for HA adsorption can be obtained at short time period (several minutes) using synthetic zeolite A, which exhibited the superiority in

comparison with natural zeolite in relation with the adsorption capacity for HA.

4. Conclusions

In this study nano-sized synthetic zeolite A was prepared simply using natural clinoptilolite rich tuff precursor.

The structure, morphology and associated property changes were studied in comparison with natural zeolite. Beside the clinoptilolite presence, zeolite LTA and sodalite forms were identified in synthetic zeolite by XRD. A lower Si/Al ratio was determined for synthetic zeolite in comparison with natural one (1.14 versus 4.5). Some changes of the zeolitic structure and water were found from FT-IR spectra for synthetic zeolite in comparison with natural one. The synthetic zeolite exhibited a more uniform structure with smoother edged lamellar crystals versus natural zeolite.

The experimental results regarding the comparative adsorption capacities of natural and synthetic zeolite for humic acid (HA) removal from aqueous solution showed that the synthetic zeolite exhibited a great capacity for HA adsorption from water.

These exploratory experiments show the feasibility of this simple synthesis method in the area of nano-sized zeolite with enhanced sorption property for humic acid envisaging water treatment. The results are part of on-going investigations in our laboratory aimed at developing zeolite-based composite materials.

Acknowledgements

The research presented in this paper is supported by the Sectoral Operational Programme Human resources Development (SOP HRD), financed from the European Social Fund and by the Romanian Government under the contract number POSDRU/89/1.5/S/63700 and by the strategic grant POSDRU/89/1.5/S/57649, Project ID 57649 (PERFORM-ERA).

References

[1] L. V. Inglezakis, H. Grigoropoulou, J. Hazard. Mater. **B112**, 37 (2004)
[2] H. Kazemian, H. Modarress, M. Kazemi, F. Farhadi, Powder Technol. **196**, 22 (2009).
[3] H. R .Tashauoei, H. Movahedian Attar, M. Kamali, M. M. Amin, M. Nikaeen, Int. J. Environ. Res. **4**, 491 (2010)
[4] L. Curkovic, S. Cerjan-Stefanovic, T. Filipan Water Res. **31**(6), 1379 (1996)
[5] H. Faghihian, S.R.Bowman, Water Res. **39**, 1099 (2005)
[6] D. A. Vujakovic, R. M. Tomasevic-Canovic, S. A. Dakovic, T.V. Dondur, Applied Clay Science **17**, 265 (2000)
[7] C. Rosa Oliveira, J. Rubi, Materials Research **10**, 407 (2007)
[8] S. Wang, Y. Peng, Chemical Engineering Journal **156**, 11 (2010)
[9] A. M. Giasuddin, S. Kanel , H. C hoi , Environ. Sci. Technol., **41**, 2022 (2007)
[10] S. Wang, T. Terdkiatburana, M.O. Tade, Sep. Purif. Technol. **62**, 64 (2008)
[11] B. Concepcion-Rosabal, G. Rodrıguez-Fuentes, N. Bogdanchikova, P. Bosch, M. Avalos, V. H. Lara, Microporous Mesoporous Mater. **86**, 249 (2005)
[12] C. Orha, F. Manea, C. Ratiu, G. Burtica, A. Iovi, Environmental Engineering and Management Journal **6**, 541 (2007)
[13] M. Rivera-Garza, M.T.Olguin, I. Garcia-Sosa, D. Alcantara, G.Rodriguez-Fuentes, Microporous Mesoporous Mater., **39**, 431 (2000)
[14] A. Jentys, J.A. Lercher, Stud. Surf. Sci. Catal. **137**, 345 (2001)
[15] H.G. Karge, Micro. Meso. Mater. **22**, 547 (1998)
[16] K. Hussaro, S. Douglas, N. Cheamsawat, American Journal of Environmental Sciences **4**, 666 (2008)
[17] W. Mozgawa, J. Mol. Struct. **596**, 129 (2001)
[18] C. Blanco, F. Gonzalez, C. Pesquera, I. Benito, S.Mendioroz, J. Pajares, Spectr. Lett **22**, 659 (1989)
[19] H. Faghihian, N. Godazandeha, J. Porous Mater. **16**, 331 (2009)
[20] D. Zhao, Jie Zhou, Ning Liu, Appl. Clay Sci. **33,** 161 (2006)
[21] P.O. Fritz, J. H. Lunsford, J. Catal. **118**, 85 (1989).

*Corresponding author: haiduccorina@yahoo.com